

## Remifentanil administration reveals biphasic phMRI temporal responses in rat consistent with dynamic receptor regulation

Christina H. Liu,<sup>a,b</sup> Doug N. Greve,<sup>a,b</sup> Guangping Dai,<sup>a,b</sup>  
John J.A. Marota,<sup>a,c</sup> and Joseph B. Mandeville<sup>a,b,\*</sup>

<sup>a</sup>MGH/MIT/HMS Athinoula A. Martinos Center for Biomedical Imaging, Massachusetts General Hospital, Boston, MA, USA

<sup>b</sup>Department of Radiology, Massachusetts General Hospital, Boston, MA, USA

<sup>c</sup>Anesthesia and Critical Care, Massachusetts General Hospital, Boston, MA, USA

Received 14 October 2005; revised 4 October 2006; accepted 17 October 2006  
Available online 13 December 2006

Many pharmacological stimuli influence multiple neurotransmitter systems in the brain, and the dynamics of the functional brain response can vary regionally. In this study, the temporal response of cerebral blood volume (CBV) was employed to spatially segment cerebral effects due to infusion of a potent mu-opioid receptor agonist. Repeated intravenous injection of 10  $\mu\text{g}/\text{kg}$  remifentanil in rats caused reproducible regional positive, negative, and biphasic changes in CBV. Three temporal processes were identified in the cerebral response and analyzed within the framework of the general linear model. Firstly, a slow component identified CBV changes that were almost exclusively negative, and the spatial distribution was similar to the inhibition produced by morphine (200  $\mu\text{g}/\text{kg}$ ). The largest CBV reductions occurred in caudate, accumbens, ventral hippocampus, cingulate, and piriform cortex. Secondly, a more rapid temporal component corresponded primarily with a regional distribution of positive changes in CBV consistent with GABAergic inhibition of hippocampal interneurons and associated projections. Thirdly, a response with the dynamics of mean arterial blood pressure correlated positively with CBV changes in hypothalamus, consistent with a central mechanism for control of blood pressure. We propose that the dominant source of the temporal variance in signal is dynamic modulation of drug targets by receptor endocytosis, an established effect *in vitro*. These results suggest that the temporal response of fMRI signal reflects underlying neurobiological processes, so that temporal decomposition strategies may aid interpretation of pharmacological mechanisms by identifying interconnected regions or those associated with common neural targets and processes.

© 2006 Elsevier Inc. All rights reserved.

### Introduction

Pharmacological stimuli possess enough dissimilarity in mechanisms of action, potential confounds, and acquisition and analysis strategies that the moniker “phMRI” is sometimes used to differentiate such stimuli from routine fMRI (Chen et al., 1997; Leslie and James, 2000). While phMRI lacks the specific information provided by complimentary PET binding techniques, it can provide information about changes in brain function with a temporal resolution unmatched by PET. Since early MRI studies of the cerebral response to acute injection of drug in humans and animal models, it has been apparent that the dynamics of phMRI signal can vary regionally for drugs like cocaine that impact multiple neurotransmitter systems (Breiter et al., 1997; Marota et al., 2000). Previous methods that have attempted to model regional variations in temporal kinetics include nonlinear fitting using a pharmacologically motivated model, together with multivariate selection criteria (Bloom et al., 1999), and clustering based upon similarity criteria after analyzing responses using a wavelet basis set (Whitcher et al., 2005).

During the past several years, it has become increasingly clear from *in vitro* studies that cerebral drug targets are regulated dynamically during exposure to drug. Up-regulation of the synaptic concentration of dopamine transporters has been reported within 1 min following application of amphetamine or cocaine (Johnson et al., 2005). Agonist-dependent modulations of receptor expressions for GABA (gamma-aminobutyric acid) and glutamine on cell membranes have been reported on a time scale of several minutes (Goodkin et al., 2005). A rapidly expanding literature on receptor trafficking suggests that these mechanisms provide dynamic control over the cerebral response to a drug (van Rijnsoever et al., 2005). Hence, it is reasonable to hypothesize that temporal responses to a pharmacological stimulus might contain information to enable segmentation of brain regions according to neural target densities and associated circuits. With that perspective, the signal dynamics in each voxel should

---

\* Corresponding author. Massachusetts General Hospital, Building 149, Room 2301, 13th Street, Charlestown, MA 02129, USA. Fax: +1 617 726 7422.

E-mail address: jbm@nmr.mgh.harvard.edu (J.B. Mandeville).

Available online on ScienceDirect (www.sciencedirect.com).

represent a summation of a few dominant temporal processes. Mathematically, the framework for handling multiple simultaneous responses is well known and commonly employed for fMRI; this is the general linear model (GLM) (Hamilton, 1994; Friston et al., 1995; Worsley et al., 2002).

This study investigates the cerebral response to two mu-opioid receptor (MOR) agonists, remifentanyl and morphine, with an emphasis on utilizing the regional dynamics of signal evolution to spatially segment the response within a statistically coherent framework in order to extract biological information about signal origins. These and other MOR agonists (e.g., heroin, oxycontin, fentanyl and its analogs) produce behavioral effects including analgesia, euphoria, progressive tolerance, addiction, and withdrawal after cessation of prolonged usage. As such, understanding the cerebral effects of these drugs is an important goal for pain research and treatment of drug addiction. Functional MRI in rats using restricted brain coverage has produced disparate results for this class of drugs. Morphine has been reported to induce positive changes in BOLD signal (Shah et al., 2005), in apparent contradiction with decreased glucose metabolism observed in another study (Cohen et al., 1991). Heroin produced predominantly negative changes in BOLD signal, with some positively responding voxels in cortex (Xi et al., 2002). In humans, a recent study of the acute effects of remifentanyl reported regional positive increases in BOLD signal with no indication of BOLD decreases (Leppa et al., 2006), whereas positron emission tomography found regional increases and decreases in cerebral blood flow (Wagner et al., 2001).

Remifentanyl, a synthetic MOR agonist that is rapidly metabolized by non-specific esterases in the blood (Patel and Spencer, 1996), was selected for this study due to its remarkably short blood half-life and cerebral effects, which enable on-off paradigms of the type traditionally employed by fMRI. Morphine, from which the MOR derives its name, was selected for comparison due to the extensive research history on this drug. A preliminary description of this work was presented in abstract form (Mandeville et al., 2005).

## Methods

### *Animal model and drug paradigm*

Descriptions of the basic rodent fMRI model have been reported previously (Marota et al., 2000). Briefly, all data presented in this study were acquired in mechanically ventilated, halothane anesthetized rats with continuous monitoring of blood pressure, oxygen saturation, heart rate, and periodic sampling of arterial blood gases. Following surgery, 0.75% halothane was maintained throughout the study. Paralysis was initiated with a loading dose of 2 mg/kg pancuronium followed by continuous injection of 2 mg/kg/h pancuronium in Lactated Ringer's solution at a rate of 5 ml/kg/h. Just prior to MRI, blood samples (mean  $\pm$  standard error of the mean) reported pH of  $7.38 \pm 0.01$ , PaCO<sub>2</sub> of  $41.9 \pm 1.6$ , and PaO<sub>2</sub> of  $129 \pm 5$ . At the conclusion of the MRI session, these values were  $7.38 \pm 0.01$ ,  $38.5 \pm 2.9$ , and  $145 \pm 3$ . The basal mean arterial blood pressure (MABP) was  $106 \pm 4$  mm Hg.

Doses and infusion rates for remifentanyl and morphine were selected based upon literature values and initial investigations in our model to assess the cerebral response and systemic effects. During initial training sessions for remifentanyl self-administration in rats (Panlilio and Schindler, 2000), rapid bolus doses up to

8  $\mu$ g/kg were employed, and trained rats performed the most bar presses for a dose of about 16  $\mu$ g/kg. To test the functional response to remifentanyl in 2 rats, we chose a unit dose of 10  $\mu$ g/kg, and we interleaved infusion rates of 5, 20, 5, 20, 2, and 2  $\mu$ g/kg/min at infusion durations of 2, 0.5, 2, 0.5, 5, and 5 min, respectively. The short (0.5 and 2 min) infusions were separated by 15-minute intervals, and long infusions (5 min) were separated by a 20-minute interval. The order of the short and long infusion paradigms was switched in the two sessions to reduce bias from injection order.

For all subsequent studies ( $n=7$ ), we infused 10  $\mu$ g/kg remifentanyl over 2 min; this was repeated every 15 min for a total of 4 injections. On average, MABP dropped about 25% during the first injection and about 10% by the fourth injection. Following this first MRI run, the catheter dead space (2  $\mu$ g/kg remifentanyl) was flushed, and a second run began 20 min later. In the second run, 200  $\mu$ g/kg morphine was injected over 45 s, and this was repeated 30 min after the first injection. The dose of morphine was selected to roughly equalize changes in MABP with those of the remifentanyl dose used in this study. MABP dropped 15–20% on each injection.

All drug stimuli were injected into a femoral vein in a volume of 1 ml/kg, so that the injected volume should not exceed 2% of total systemic blood volume, assuming a 5% systemic blood volume fraction. Small injection volumes reduce transient signal changes due to hemodilution.

### *MRI data acquisition*

Data were collected at a magnetic field of 4.7 T using an elliptical surface coil (30 mm by 20 mm) for transmission and receptor of radio frequency power, a field of view of 30 mm, a two-dimensional image matrix of  $96^2$  with 20 contiguous slices of 1 mm to cover rat brain, and 16-shot gradient echo planar imaging with a repetition time of 625 ms, an echo time of 10 ms, and an excitation power set to optimize signal strength. The temporal resolution per brain volume was 10 s.

Studies employed the iron oxide contrast agent MION (monocrystalline iron oxide nanocompound) to enhance functional sensitivity and spatial localization since this method has a much higher contrast to noise ratio (CNR) than BOLD signal below 10 T (Mandeville et al., 2004). Data are reported as the percentage change in CBV, which can be calculated at any voxel using signal changes due to drug infusion together with the signal change due to injection of MION contrast agent prior to the functional acquisition (Mandeville et al., 1998, 2004). The term “fCBV” is used to denote a functional change in CBV within a voxel or region, so as to distinguish this relative measurement from absolute CBV and from relative regional CBV, which is commonly referred to as “rCBV” in the MRI literature.

### *Subject alignment and regions of interest*

Subject data were aligned to the stereotactic coordinate of Paxinos and Watson, which was estimated by the authors to be accurate within a tolerance of 500  $\mu$ m (Paxinos and Watson, 1998). To provide the reference frame, 42 coronal slices of the digital atlas at 500  $\mu$ m separation intervals were down-sampled to an in-plane resolution of 25  $\mu$ m, and the 1 mm grid lines of the stereotactic atlas were aligned with grid lines of our software coordinate system. To provide an average MRI template, fast spin-echo T2-

weighted images were acquired for anatomical detail using 2-dimensional slice-selective MRI with 44 slices at 500  $\mu\text{m}$  separation intervals with an in-plane resolution of 230  $\mu\text{m}$ ; these images were resampled to 250  $\mu\text{m}$  resolution in the image plane, and data were averaged across rats by maximizing the mutual information (Holden et al., 2000) using a standard affine transformation with 12 degrees of freedom (3 translations, 3 rotations, 3 inflations, and 3 skews). Additionally, gradient echo planar images prior to and after injection of MION contrast agent were collected in each session in order to provide templates for subsequent cross-subject alignment.

Subject-averaged volumetric images were manually aligned with the Paxinos–Watson atlas using 12 degrees of freedom by direct superposition using a 10 to 1 pixel ratio in the image plane. Registration between the atlas and the MRI template images appeared to be excellent, except at slice locations more anterior than 4.2 mm with respect to bregma. At the most anterior aspect of the Paxinos–Watson atlas (6.2 mm relative to bregma), the Paxinos–Watson atlas differed from the MRI template by 1.75 mm. This misalignment probably represents deformation of the Paxinos–Watson atlas due to gravity after removal of brain from the skull, so care should be employed when relying up these coordinates in the region of the olfactory bulb. After creation and alignment of the template images, all subject data in this manuscript were automatically aligned to the template data using maximization of mutual information as previously described.

Regions of interest were defined by manually tracing anatomical areas on the Paxinos–Watson Atlas using Bezier curves on each of the 42 slices to define wire frames for presentation and to define closed regions, which were then converted to binary bitmaps at a resolution of  $25 \times 25 \times 500 \mu\text{m}$ . These bitmaps were converted to non-binary overlays by down-sampling to a resolution of  $250 \times 250 \times 1000 \mu\text{m}$  resolution. This method provides a means to account for partial-volume effects in three dimensions due to the lower resolution of the MRI data.

To increase the robustness of subject results and mitigate errors in cross-subject alignment, all data were spatially smoothed in the image plane using a Gaussian filter with a full width at half maximum of 500  $\mu\text{m}$ . All gray-scale images presented in figures are subject-averaged, post-MION gradient echo planar images

from the functional data sets. Slice locations with respect to bregma are indicated in the lower right corner of each panel. Tick marks on image panels show 2 mm steps; the top tick mark in the dorsal–ventral direction represents the level of bregma in that dimension.

### Statistical analysis

Functional responses were analyzed within the standard GLM framework. Temporal data ( $y_t$ ) can be represented within a design matrix ( $X_{te}$ ) as a linear summation of time-dependent basis functions multiplied by scaling factors ( $\beta_e$ ) in order to describe data within the limits of noise:  $y_t = X_{te}\beta_e + n_t$  (Hamilton, 1994; Friston et al., 1995; Worsley et al., 2002). Statistical inference can be assessed by a  $t$  test for a specified linear combination of parameters, or by an  $F$  test for multiple such combinations.

Fig. 1 shows a simplified multi-compartment model with first-order rate constants to motivate the choice of basis functions used for analysis in this report and to describe the hypothesis underlying observed temporal differences in our MRI data. For this simple system, solutions can be obtained numerically or analytically. The figure assumes an instantaneous bolus of drug, followed by mono-exponential decay in the plasma. Pharmacokinetic models generally describe plasma drug concentration with a bi-exponential decay accounting for redistribution of drug to a generalized peripheral compartment plus systemic elimination of drug. However, measured blood concentrations of remifentanyl in the rat exhibit rapid, single exponential decay (Haidar et al., 1997).

Within this framework, the brain concentration of drug has an initial slope proportional to the wash-in rate ( $K_{IN}$ ), and the temporal evolution of drug availability in the brain can be represented as a difference of exponentials with rate constants set by drug elimination ( $K_E$ ) and wash-out from the brain ( $K_{OUT}$ ). If drug availability solely determined the pharmacodynamics of brain activation, all regions in the brain would exhibit the same temporal profile of response. However, modulation of brain function is determined both by drug availability and efficacy upon the target protein (receptor or transporter), which may also respond dynamically. The figure depicts a homeostatic down-regulation of the response through feedback, which effectively increases a composite wash-out/offset rate and

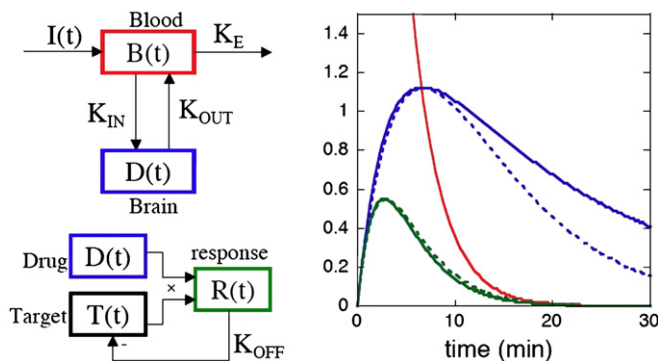


Fig. 1. Left: a multi-compartment model describing the blood and brain concentrations of drug, plus potential feedback that is specific to the cerebral target. Rates specify elimination of drug from the plasma ( $K_E$ ), transfer across the blood brain barrier ( $K_{IN}$  and  $K_{OUT}$ ), and a system-specific offset rate ( $K_{OFF}$ ) that returns activity of the binding target toward baseline even in the presence of drug. Right: analytic solutions (solid lines) for a rapidly delivered bolus of drug that is eliminated from the blood with mono-exponential kinetics (red) and that washes into and out of the brain with equal time constants ( $K_{IN}=K_{OUT}$ ). A system that down-regulates activity in the presence of drug ( $K_{OFF} \neq 0$ ) has a more rapid return to baseline than one that follows the drug concentration in the brain ( $K_{OFF}=0$ ). Dashed lines depict gamma-variate functions employed as approximate impulse responses within the general linear model.

thereby shortens the time to peak response and the return to baseline. Receptor internalization is one potential mechanism to dynamically down-regulate the response. The important point is that regional differences in cerebral dynamics cannot occur without regional differences in target dynamics or by mechanisms that temporally modify the response during continued binding of drug and target.

Because we delivered drug over an extended time window, rather than as an instantaneous bolus, we generated regressors for GLM analyses by convolving an input function with impulse response functions (IRFs). As an input function for convolution with the IRFs, we used the infusion paradigm in the same way as traditional fMRI analyses use the stimulation paradigm. Note that scaling the input function by the infusion rate in this method makes the assumption that brain activation increases linearly with the dose of drug, which generally is not true across a wide dose range.

As an alternative method, one can move one step closer to the brain by replacing the infusion paradigm with an estimate of the blood plasma concentration of drug, as suggested by Fig. 1. For the latter method, the blood plasma concentration can be computed using a mono-exponential decay approximation by convolving the injection paradigm with an exponential decay function, and then basis functions for the GLM analysis can be generated using a second convolution of IRFs with the blood plasma profile. For analyses of these data, we tested this double convolution method using the reported blood half-life for remifentanyl in the rat of 40 s (Haidar et al., 1997), but results were not obviously better than a single convolution of the infusion paradigm with response functions. Hence, all results employed the infusion paradigm as the input function without estimating the blood plasma temporal profile.

As IRFs, we employed simple gamma-variate functions of the form  $x \exp(-x)$ , where  $x=(t-T_0)/\tau$  describes an instantaneous injection at time  $T_0$  with a shape determined by the single time constant  $\tau$ . As depicted in Fig. 1 (dashed lines), such functions provide a good approximation of the modeled temporal profiles through the peak of the response. Additional parameters could be used to refine the shape of the tail, but this information can be obscured by baseline drift, and there is no guarantee that the simple first-order model description is accurate. The peak responses of all gamma-variate basis functions were normalized to unity, so that all functional tests compare peak amplitudes (as opposed to integrated area, for instance).

In addition to the analysis based upon gamma-variate IRFs, we performed a finite impulse response (FIR) analysis on both the remifentanyl and morphine data. FIR analyses are “unbiased” in the sense that they do not assume a functional form for the model. This analysis was employed in order to search for regional responses that did not conform to our IRF model, as well as to provide a comparison for the IRF model in terms of the global residue and statistical power of the respective fits. In this analysis (Figs. 2c, d), data were fit as a series of 9 block intervals of 1 min each, so that the magnitude of each square function was determined from 24 data points in each subject (6 points per regressor times 4 stimuli) and averaged across 7 subjects.

Due to uncertainties in model identification, temporal correlations in the “noise” (i.e., the residual between the data and the fit) can be expected to have a different structure for phMRI relative to fMRI analyses. fMRI analyses typically describe temporal correlations using autoregressive models of low order (AR( $n$ )), which assume that each time point has some dependence on the  $n$

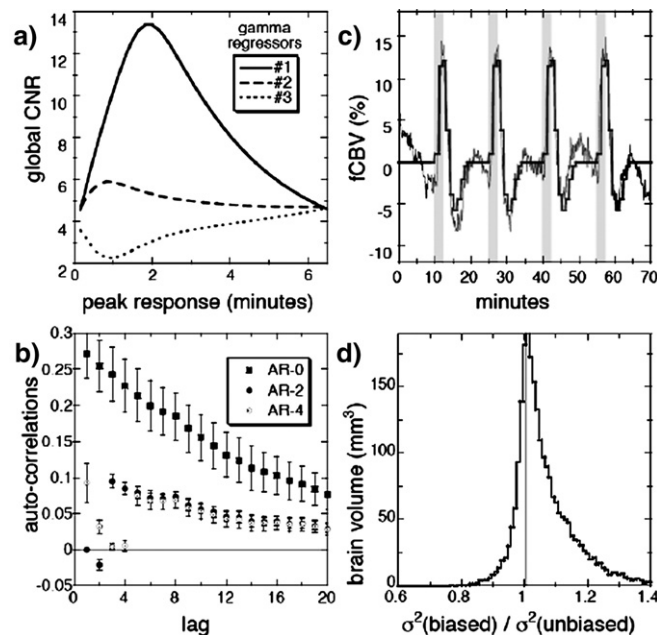


Fig. 2. (a) A series of successive one-dimensional searches identified the optimal response functions to describe the remifentanyl data by maximizing the global contrast to noise ratio (CNR) determined by a  $t$  test for each regressor. (b) When 3 gamma-variate regressors were employed to describe the remifentanyl data ( $n=7$ ), a second-order autoregressive model (“AR-2”) of the noise reduced the global average autocorrelations below 0.1 for all temporal lags. (c) An “unbiased” finite impulse response (FIR) analysis using sequential block regressors of 1-minute duration, as shown in dorsal hippocampus, provides a comparison for the “biased” impulse response method based upon gamma-variate functions. Light lines are subject-averaged data, and dark lines shown the FIR fit. (d) The biased analysis produced a global distribution of residual variance nearly as small as the FIR (“unbiased”) analysis. The panel shows a histogram of the ratio of residual variances and includes all voxels that reached significance by either analysis.

previous time points. Autocorrelations in the noise at each voxel were assessed and then reduced using the procedures described by Worsley et al. (2002). Autocorrelations of residuals were computed at each voxel, and then correlations coefficients were smoothed spatially using a 1 mm Gaussian kernel. Subsequently, the data and GLM model were pre-filtered with a whitening matrix on a second pass through the data.

All functional maps show results of fixed-effects analyses and employ a  $p$ -value threshold of 0.05, after correction for multiple comparisons by the method of Gaussian random fields (Worsley et al., 2004). Temporal analyses are presented as an average across subjects, although actual analyses were performed using the usual method of concatenating subject data in order to individualize aspects of the analysis like the MABP regressor. Temporal data are shown after removal of baseline drift, which was fit in the GLM using a second-order polynomial, and error bars reflect the standard error of the mean across subjects. CNR was calculated as the square root of the  $F$  statistic. Regions of interest, as defined from the Paxinos–Watson atlas, were considered significant using a random effects model (one observation per regressor per subject) with a false positive rate of 5%.

## Results

### Analysis model

Remifentanyl produced obvious, repeatable biphasic responses throughout the hippocampus and numerous other regions. In order to analyze the response using a biologically motivated framework, as described in Fig. 1, at least two temporal processes must contribute. To determine the number and shape of the contributing processes, global CNR was maximized in a series of sequential one-dimensional searches, as illustrated by Fig. 2a. Using a single gamma-variate impulse response function, a time-to-peak of 2 min in the gamma-variate IRF maximized global CNR. When this regressor was included in conjunction with a second IRF, the global CNR for the second process was maximized at a time-to-peak of 1 min. A third regressor found a local CNR maximum at very short times. Rather than employ a very rapid impulse response function as a third regressor, we instead substituted recorded values of MABP, which exhibited similarly rapid temporal dynamics. Additionally, the global CNR for the third term slowly increased monotonically as a function of peak response time up to the inter-stimulus interval of 15 min (not shown). Such long response functions produce slight modifications to the descriptions of both baseline drift and the response shape, so this effect was ignored.

Two methods were employed to assess the model. Firstly, we measured autocorrelations in the residue between the data and fit. When no stimuli were employed in an MRI session ( $n=1$ , not shown), the first-order global autocorrelation coefficient was 0.15, but pre-whitening the data and GLM model using an AR(2) procedure was sufficient to reduce global autocorrelations of all orders below  $\pm 0.05$ . When analyzing phMRI data, imperfections in the model fit can introduce additional autocorrelations in the residue. The average first-order global autocorrelation coefficient was 0.25 (Fig. 2b), and an AR(2) model reduced all autocorrelations below 0.1, but higher order autocorrelations were consistently nonzero. An AR(4) model showed similar results for the high order coefficients. This tail of high order autocorrelations may reflect non-stationary temporal correlations in the residue due to imperfections in the model (see fits in Fig. 7).

Temporal autocorrelations do not bias the mean response magnitudes of coefficients within a GLM analysis, but they can bias the variance of the coefficients across subjects (Worsley et al., 2002), such that analyses that do not properly account for autocorrelations will not have optimal detection power. In terms of cross-subject results, this was found to be a minor effect. The cross-subject variance of an AR(0) analysis was greater than that for an AR(2) or AR(4) analysis in each of 40 regions tested, but the average increase of the standard deviation across subjects was only about 5% for the regressors employed in the remifentanyl analysis. Cross-subject variances were identical for the AR(2) and AR(4) analyses. All subsequent analysis employed an AR(2) procedure.

An FIR methodology, which does not assume any shape for the response in each voxel, provides a second way to assess the fit of the model through a comparison of residual variances. Fig. 2c shows the data and FIR fit in dorsal hippocampus. Fig. 2d demonstrates that the “biased” analysis based upon gamma-variate IRFs provides a distribution of residual variances across whole brain comparable to an “unbiased” FIR analysis.

The procedure shown in Fig. 2a was applied also to the morphine data, and two regressors were included in the analysis for that drug. The response to morphine was largely described by a single impulse response function that peaked at 6 min, and an additional weak response was found with a time constant that matched MABP.

To test the IRF methodology and assess the linearity of the response versus infusion rate for remifentanyl, we varied the injection rate using a constant injection volume and concentration of drug ( $n=2$ ). The top panel of Fig. 3 depicts the infusion paradigm, with magnitudes representing infusion rates (5, 20, 5, 20, 2, 2  $\mu\text{g}/\text{kg}/\text{min}$ ) for these injection durations (2, 0.5, 2, 0.5, 5, 5 min). Two response profiles (middle panel) were defined by convolving the infusion paradigm with the two impulse response functions as described previously, and then the time course of each

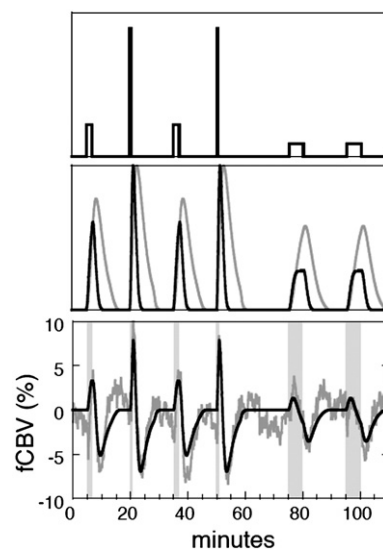


Fig. 3. Top: an infusion paradigm for remifentanyl, with height indicating infusion rate. Middle: two impulse response functions were convolved with the infusion paradigm to represent two distinct temporal processes within an analysis based upon the general linear model. Bottom: the general linear model produces a good fit (black) to the CBV response of whole hippocampus (gray,  $n=2$ ).

voxel was modeled with the GLM framework as a simple summation of these basis functions, plus three baseline drift terms per run. The bottom panel depicts data from whole hippocampus (gray) and the GLM estimate (black). It can be seen that the resulting GLM fit produces a reasonable description of the biphasic data in the hippocampus for this infusion protocol.

#### Functional responses

Fig. 4 shows the response of rat brain to four repeated injections of 10  $\mu\text{g}/\text{kg}$  remifentanyl ( $n=7$ ) using an  $F$  statistic to determine significance for either of the two temporal components of signal change (the blood pressure regressor is excluded in this statistical test but will be revisited later). Panels show brain slices from 3.2 to  $-13.8$  mm with respect to bregma. The color overlay defines the regional contrast to noise ratio, with red–yellow colors indicating positive changes and blue–green colors indicating negative changes. Where positive and negative changes both reached significance (e.g., biphasic response), this map shows the largest magnitude of the two components. Generally, negative changes predominate

throughout brain, although positive changes were largest in dorsal hippocampus, posterior entorhinal cortex, cerebellum, and ventral posterior lateral thalamus.

The temporal components of MRI signal can segment the response to remifentanyl. Fig. 5 compares the spatial distribution of the slow response of remifentanyl to the response of morphine in terms of the magnitude reduction of fCBV, using a three-fold smaller scale for morphine. No regions responded positively for morphine, and only ventral tegmentum area (VTA) responded with a significant positive slow temporal component for remifentanyl when analyzed across subjects using a random-effects model. The figure shows a coronal brain slice at the level of basal ganglia, and a horizontal slice 4.5 mm ventral to bregma. For reference, white lines trace anterior cingulate, caudate, septum, piriform cortex, and the core of the nucleus accumbens. The overall patterns of fCBV reduction for morphine and the slow component of fCBV were remarkably similar, with the largest reductions found in caudate, accumbens, hippocampus (particularly the ventral portion), cingulate, and piriform cortex. Graphs show the subject-averaged time data for whole caudate for both drugs, with points binned to one-minute intervals for display.

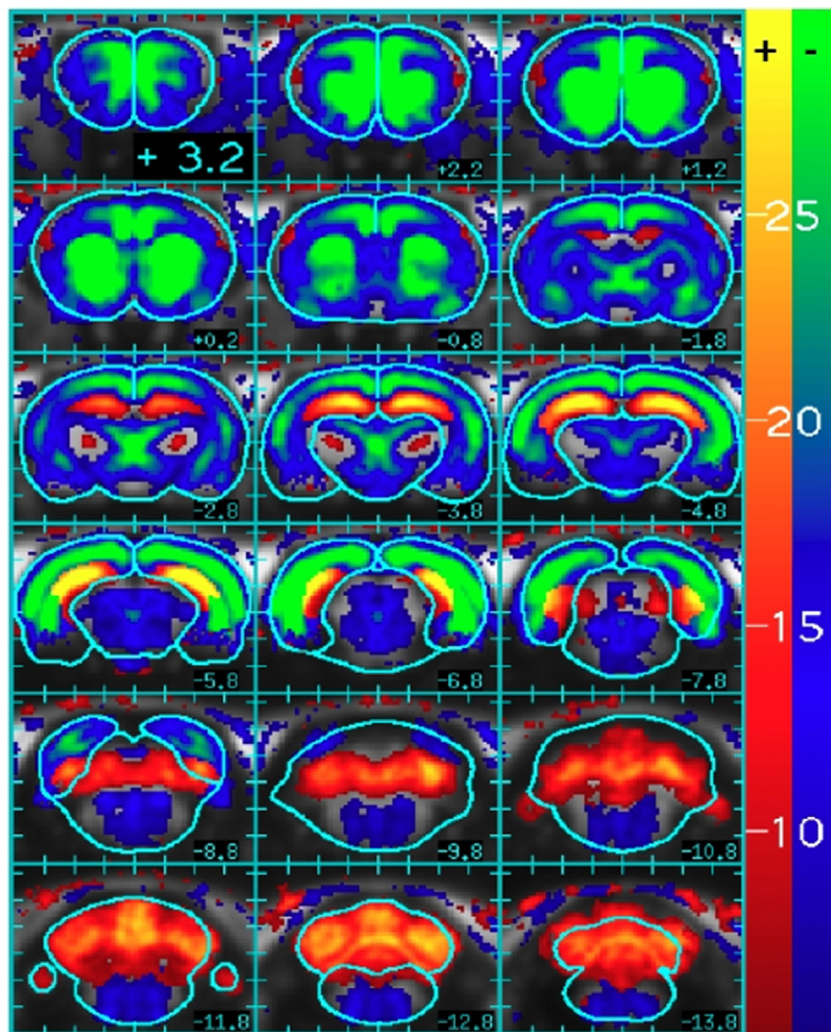


Fig. 4. The contrast to noise ratio (square root of  $F$  statistic) for changes in CBV due either to the slow or rapid components employed in the analysis of the remifentanyl response (10  $\mu\text{g}/\text{kg}$ ,  $n=7$ ). The color scale is divided into positive (red–yellow) and negative (blue–green) scales, and the color at each voxel is assigned according to the largest magnitude of the two regressors. Slice locations and brain outlines are from the rat stereotaxic atlas (Paxinos and Watson, 1998).

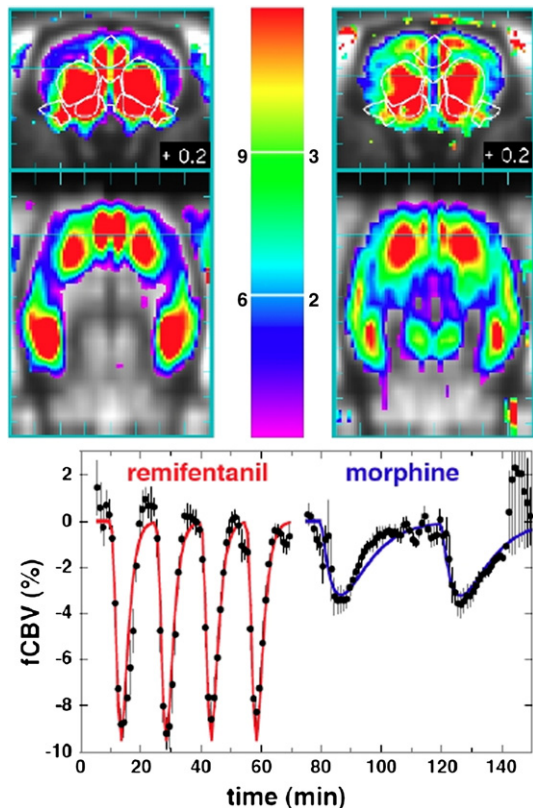


Fig. 5. Top: the negative magnitude of the slow response to 10 µg/kg remifentanil (left) is compared to the response of 200 µg/kg morphine (right) in coronal (top) and horizontal (bottom) planes. The horizontal cyan line in each figure indicates the slice plane in the other projection. The colorbar shows the percentage reduction in CBV from 3 to 12% for remifentanil and 1 to 4% for morphine. Bottom: temporal responses in caudate for 4 injections of remifentanil and 2 injections of morphine.

Fig. 6 displays a map of the fast component of fCBV. Significant positive activation across subjects occurred throughout the hippocampus and subiculum (green outlines), rhinal cortex (purple), piriform cortex (white), portions of medial prefrontal cortex (the green outline on slice 2.2 mm anterior to bregma indicates infralimbic cortex and dorsal peduncle), and cerebellum (white), while insignificant but small reductions in fCBV occurred in VTA, (yellow), raphe (red), pontine reticular nuclei (orange), and the reticular nuclei in the caudal portions of brainstem (green, posterior slices).

The temporal response to remifentanil was variable throughout brain, but the GLM analysis described the response well in most regions. In Fig. 7, piriform cortex and caudate both exhibited a monophasic reduction of fCBV, but the analysis interpreted a temporal shift in the former region as a summation of both negative and positive contributions. Hippocampus exhibited biphasic responses in most regions. In Fig. 4, the positive and negative responses in hippocampus (e.g., slice at  $-5.8$  with respect to bregma) are seen to be equal at about 5 mm ventral to bregma, and this level was used to divide dorsal and ventral portions for Fig. 7. Rapid positive changes exceeded the slower negative response in dorsal hippocampus, whereas slow negative changes predominated in the ventral hippocampus. In fact, the slower negative temporal component produced a progressively larger contribution along the dorsal–ventral axis of hippocampus, such that the response in the

most ventral aspect of hippocampus was a monophasic reduction of fCBV with a temporal shift relative to the slow regressor, similar to the response in piriform cortex. Although most large changes in the rapid component of fCBV were positive, the VTA (as shown in Fig. 7), the reticular nuclei in brainstem, and raphe were among the regions with biphasic responses that initially went negative. It should be noted that some regions were not fit particularly well by this analysis; cerebellum (see figure) and central thalamic nuclei fall into this category.

MABP was recorded for inclusion in the GLM analysis in order to remove spatially non-specific “effects of no interest” in fCBV due to autoregulation of blood flow, as well as to identify regions potentially associated with central regulation of blood pressure. Averaging across repeated injections of remifentanil and morphine, the distribution of signal changes throughout whole brain was well described by a Gaussian function with a mean and standard deviation of  $-0.8 \pm 2.7\%$  fCBV, and the largest negative correlation between MABP and fCBV ( $-0.17\%$  fCBV per mm Hg) was observed in the caudate. Interestingly, fCBV correlated positively with MABP in the hypothalamus (Fig. 8), a region important for homeostasis of systemic physiological functions, including regulation of MABP. fCBV dropped as rapidly as MABP, but then it returned to baseline about 1 min sooner than MABP. A secondary analysis defined MABP tracings for remifentanil and morphine as separate events with a GLM analysis in order to look for spatial differences in the response, but differences did not reach significance.

## Discussion

This study employed remifentanil, an analog of the MOR agonist fentanyl, because its rapid temporal profile is ideal for a pharmacological probe using phMRI within this important class of addictive analgesics. Results demonstrated a complex cerebral response, including increases and decreases in fCBV, and regional variations in the temporal response. However, the response was described well across whole brain with two simple temporal components, plus MABP as an additional objective regressor. We argue that the two impulse response functions represent generalized inhibition and GABA-mediated indirect excitation and that temporal differences between these processes are most likely a result of dynamic receptor internalization, as observed *in vitro*. The anatomical pattern produced by the individual temporal components provides a compelling case for the biological relevance of such segmentation techniques based upon the temporal response to a drug, and this method should be widely applicable and informative in analyses of numerous other drugs using functional MRI.

### Spatial distribution of fCBV changes

Extensive *in vitro* studies of opiate mechanisms have shown that endogenous and exogenous MOR agonists reduce calcium conductance and increase potassium conductance, leading to neuronal inhibition due to reduced neurotransmitter release (Di Chiara and North, 1992; Vaughan et al., 1997). The highest regional MOR densities are found in caudate, hippocampus, and several thalamic nuclei (Diaz et al., 2000), so the sign and spatial distribution of fCBV decreases shown in Fig. 5 for morphine and the slow component of the remifentanil response are not surprising. Accounting for the 20-fold smaller dose and 3-fold larger effect of

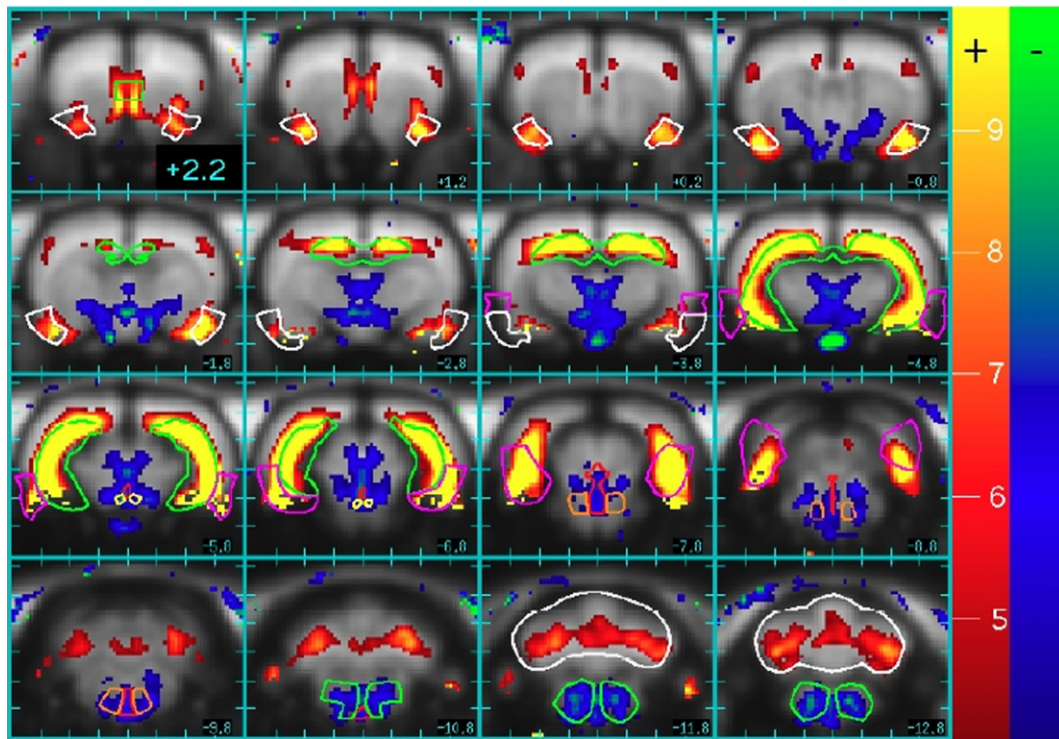


Fig. 6. Positive (red–yellow) and negative (blue–green) percentage changes in the rapid component of the CBV response due to remifentanyl. Regions of interest that reached significance across animals include piriform cortex (white, rostral slices), hippocampus (green), rhinal cortex (purple), ventral tegmentum area (yellow), raphe (red), pontine reticular nuclei (orange), reticular formation (green, caudal slices), and cerebellum (white, caudal slices).

remifentanyl relative to morphine in caudate, as shown in Fig. 5, these results demonstrate that remifentanyl is roughly 60 times more potent in its cerebral effects than morphine. This result matches the 60-fold greater analgesic potency for remifentanyl as reported for intraperitoneal injection of these drugs (Buerkle and Yaksh, 1996), although analgesia need not be modulated in cerebral regions reported here.

In addition to decreases in fCBV, remifentanyl also produced local increases in fCBV that were temporally segmented from the slower inhibitory response of Fig. 5. In particular, the fast temporal component of the response identified the entire hippocampal formation, entorhinal cortex, piriform cortex, and portions of amygdala and cerebellum (Fig. 6). Researches over the past 15 years – particularly *in vitro* studies employing brain slices – have shown that MOR agonists indirectly produce excitation of granule and pyramidal cells in hippocampus by inhibiting the inhibitory influences of GABAergic interneurons (Neumaier et al., 1988; Lambert et al., 1991; Drake and Milner, 1999; McQuiston and Saggau, 2003). Of particular relevance to our results, this indirect excitation occurs together with an inhibitory influence on synaptic currents that is revealed after pretreatment with a GABA-A antagonist to block the indirect excitation (Xie and Lewis, 1997; Xie et al., 1992). Our results are consistent with dual opposing mechanisms in the hippocampus, as shown *in vitro*. Significantly, pHMRI appears to temporally discriminate these competing influences of remifentanyl.

The set of brain structures activated through the rapid component of the remifentanyl response includes circuitry implicated in animal models of experimental epileptogenesis. For instance, piriform cortex has connections to the major input

(entorhinal cortex) and output (subiculum) centers for the hippocampus, which may explain why it is the most sensitive region in the brain to electrical stimulation as a means to generate seizure activity (Loscher and Ebert, 1996). Note that this analysis assigned a rapid temporal contribution to regions like piriform cortex and the most ventral aspects of hippocampus, even though these regions exhibited exclusively negative responses because these responses were temporally shifted relative to the slow regressor.

Although both remifentanyl and morphine are putative MOR agonists, morphine induced no positive activation in hippocampus or elsewhere. However, there are several known differences between these drugs. Blood pressure modulation limited the injected dose of morphine, which causes peripheral vasodilation through the release of histamines, an effect that is much smaller for fentanyl and its analogs (Rosow et al., 1982; Bowdle, 1998). Normalized to the respective MOR affinities for the two drugs, the relative affinity for the kappa-opioid receptor is at least 100 times greater for morphine than remifentanyl (James et al., 1991; Mignat et al., 1995). Agonists for kappa-receptors inhibit hippocampal activity by reducing glutamate release, while apparently having no effect on interneurons (Wagner et al., 1992). Thus, morphine's affinity for kappa-receptors might explain the lack of excitation seen with that drug.

Our results for morphine appear to contradict those obtained in a recent study using BOLD signal (Shah et al., 2005), but it is more difficult to relate our results to patterns of heroin-induced brain stimulation. IV heroin is metabolized to both morphine and 6-acetylmorphine, and the latter acts more like a high-efficacy MOR agonist of the fentanyl class than like morphine (Selley et al.,

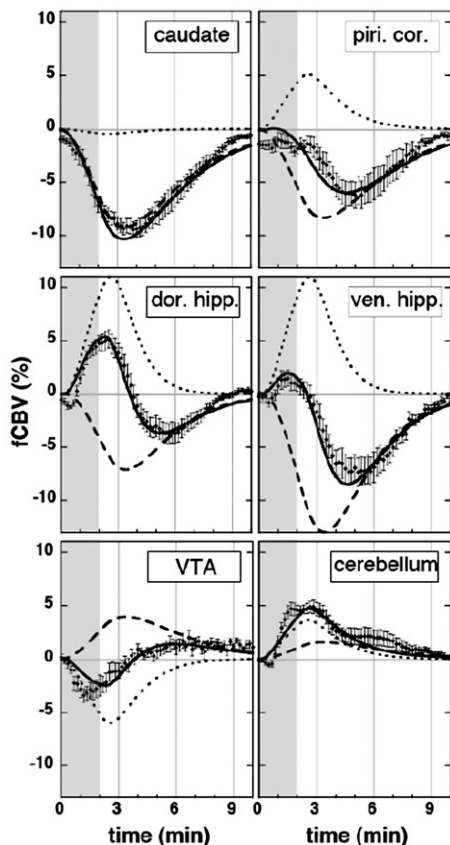


Fig. 7. Temporal responses in regions of interest (Paxinos and Watson, 1998), together with slow (dashed) and fast (dotted) regressors and the total fits (solid lines) from the general linear model analysis.

2001). Hence, IV heroin might be expected to produce a spatial profile of activity like morphine, but with some of the positive influences produced by remifentanyl. In fact, heroin produced both negative and positive changes in BOLD signal in a rat study (Xi et al., 2002). While the pattern of reported positive BOLD signal changes for heroin does not match the pattern of fCBV increases reported here for remifentanyl, we did observe small fCBV increases in lateral frontal cortex (Fig. 6) and more pronounced cortical activation in several animals, as reported in the heroin study.

#### Regional variations in the temporal response

Homeostatic feedback mechanisms have long been postulated to explain long-term consequences to opiate exposure, like tolerance and withdrawal, but only recently have studies begun to explore dynamic feedback during the acute response to drugs. Although various mechanisms could alter the neuronal response to a drug, internalization of receptors into cells provides a potentially rapid and effective means to adjust system sensitivity and thereby produce activity-dependent synaptic plasticity (Carroll et al., 2001; Kneussel, 2002). Agonist-dependent endocytosis was first observed for the GABA-A receptor, which internalized into cells at a faster rate when exposed to GABA (Tehrani and Barnes, 1991). An intracellular pool of GABA-A receptors is located just under the cell membrane in an ideal position for rapid transport to the cell

surface (van Rijnsoever et al., 2005). The basal half-life for receptor internalization *in vitro* is less than 10 min (Goodkin et al., 2005), and increased bursting activity reduced this value by about 3 min.

However, extrapolation of individual cellular measurements to the complex *in vivo* environment is not straightforward. Mechanisms for internalization may depend upon more than just the synaptic concentration of agonist (Goodkin et al., 2005). Moreover, GABA-A is not the only receptor to exhibit endocytosis *in vitro* on a time scale of minutes. Glutaminergic AMPA (alpha-amino-3-hydroxy-5-methyl-4-isoxazolepropionic acid) receptors exhibit basal endocytosis rates comparable to those for GABA-A receptors, and internalization increases with the rate of AMPA stimulation (Ehlers, 2000; Carroll et al., 2001). MORs also demonstrate agonist-induced internalization (Law et al., 2000), although there appears to be no evidence to date that it occurs on these short time scales. Thus, temporal differences observed in this study may well represent composite effects. Agonist-induced endocytosis might up-regulate available GABA receptors and down-regulate downstream glutaminergic receptors in areas dominated by GABA-mediated excitation, such as the dorsal hippocampus, and both of these processes would shorten the temporal response. Generally, the MRI data adhered to a rule whereby positive responses had a shorter time to peak, corresponding to a greater negative feedback rate (Fig. 1), than negative responses. This was not always the case, however, as illustrated by the biphasic responses in VTA and the reticular formation, for which the fast responses were negative. However, if we propose that the rapid temporal component of MRI signal change is a marker for GABAergic inhibition, then downstream effects under the influence of GABA may be either excitatory (e.g., glutamatergic) or inhibitory; inhibitory effects upon serotonin in the raphe nucleus, the principal source of serotonin release, are consistent with this hypothesis.

The temporal response in hippocampus exhibited a continuous variation along the dorsal–ventral axis, with the most dorsal regions showing a predominately fast excitatory response (Fig. 2) and the most ventral regions reacting with a monophasic decrease in fCBV. Converging lines of experimental evidence suggest a functional differentiation between dorsal and ventral hippocampus (Moser and Moser, 1998). For instance, ventral hippocampus is more susceptible than dorsal areas to seizure-like events (Borck and Jefferys, 1999). Two recent studies have addressed dorsal–ventral differentiation by mapping receptor densities, and results show more GABA-A receptors in dorsal regions (Sotiriou et al., 2005), but more glutaminergic NMDA (*N*-methyl-D-aspartic acid) receptors in ventral regions (Papatheodoropoulos et al., 2005). Our data can be interpreted to be consistent with these findings, in that excitation, which presumably occurs indirectly through GABAergic inhibition, is largest in dorsal hippocampus, whereas inhibition is largest in ventral regions.

#### Systemic physiology

Changes in blood pressure and blood gases due to drug infusion can contaminate inferences from functional imaging that are based upon flow–metabolism coupling. These studies employed mechanical ventilation to minimize changes in PaCO<sub>2</sub> because opiates are known to depress respiration, which would produce non-specific increases of blood flow, blood volume, and BOLD signal in free-breathing animals due to elevated levels of

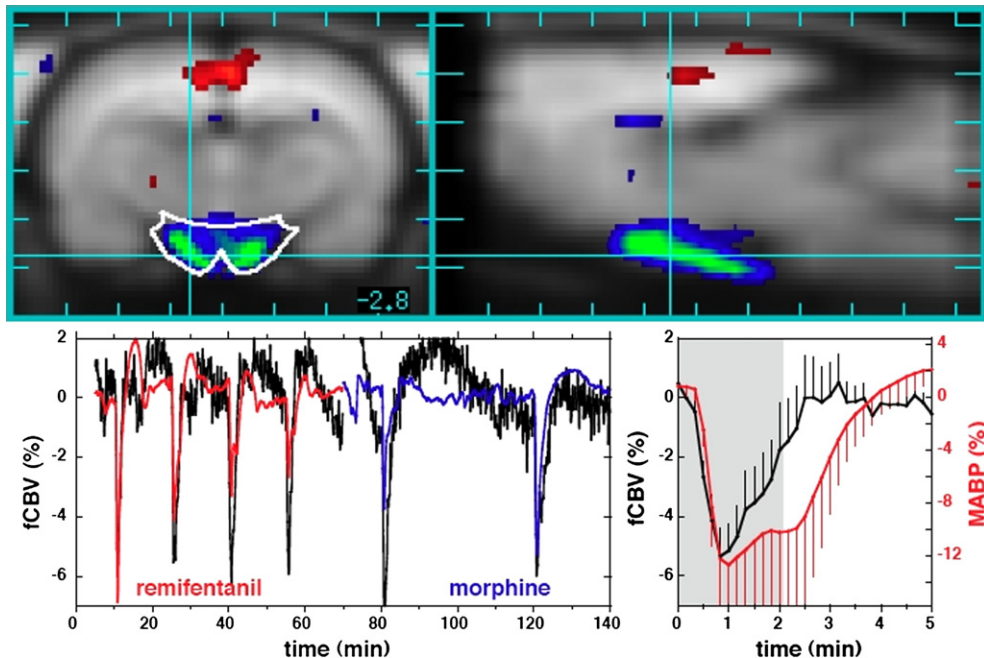


Fig. 8. Top: coronal (left) and sagittal (right) views of rat brain showing a strong positive correlation between mean arterial blood pressure (MABP) and functional changes in CBV (fCBV) in hypothalamus. However, whole brain excluding hypothalamus demonstrated a very weak negative correlation between fCBV and MABP, with an average response less than  $-1\%$  fCBV per  $10\%$  change in MABP. Bottom: MABP (red and blue) and pHMRI data (black) from hypothalamus after removing other effects (left), and the response of fCBV in hypothalamus (black) relative to MABP (red) for remifentanyl (right).

arterial carbon dioxide. A recent study in free-breathing rodents found that intraperitoneal injection of  $5\text{ mg/kg}$  morphine induced positive changes in BOLD signal (Shah et al., 2005), which could result from respiratory depression. BOLD signal is particularly susceptible to contamination by changes in arterial  $\text{CO}_2$  concentration because hypercarbia does not affect oxygen utilization; hypercarbia-induced increases in BOLD signal are roughly twice as large as those due to neuronal activation for matched changes in blood flow (Hoge et al., 1999). Autoradiographic mapping of glucose utilization in the rat found morphine-induced decreases in metabolism in all reported regions (Cohen et al., 1991), supporting the results obtained in this study using mechanical ventilation.

As reported previously for BOLD signal (Kalisch et al., 2001), global signal changes associated with blood pressure are small and difficult to detect by pHMRI. In this study, global fCBV increased by only  $1\%$  for a  $25\%$  reduction of MABP. Such small non-specific changes in blood volume across the autoregulatory range of MABP are consistent with previous MRI measurements of blood flow, fCBV, and BOLD signal during hemorrhagic hypotension in the rat (Zaharchuk et al., 1999).

Interestingly, fCBV correlated positively with MABP in the hypothalamus, a region important for homeostasis of systemic physiological functions, including regulation of blood pressure. fCBV and MABP dropped at about the same rate, but fCBV recovered to baseline more rapidly than MABP (Fig. 5). Because the average rate of pressure modulation was slower than the threshold rate of about  $24\text{ mg Hg/min}$  that has been reported for loss of autoregulation in rat cortex (Barzo et al., 1993), it is unlikely that fCBV decreases in the hypothalamus as a consequence of pressure-dependent flow. Rather, studies employing micro-injection of opioid agonists and antagonists into the

paraventricular nucleus of the hypothalamus support a central mechanism for pressure regulation via a depressor pathway that appears to occur via MOR mediated inhibition of vasopressin (Sun et al., 1996; Lessard and Bachelard, 2002).

By minimizing changes in  $\text{PaCO}_2$  and correcting for the small influences of MABP, our presumption is that fCBV is an effective surrogate for cumulative metabolic processes driven by neural activity. However, we cannot exclude possibilities that remifentanyl produces (1) spatially non-specific direct effects on vascular smooth muscle tone, which are known to accompany some anesthetic agents, or (2) regional variation in the relative vascular and neural responses, perhaps as a consequence of receptors located on endothelial cells (Stefano et al., 1995) or interneurons projecting to vessels. The regional responses reported here argue against a significant contribution from the former effect, whereas the latter observation may represent intrinsic aspects of neurovascular coupling (Iadecola, 2004). To date, there appears to be little experimental evidence for flow–metabolism “uncoupling” due to remifentanyl or related opiates.

#### Limitations of analysis methodology

To our knowledge, this is the first application of the GLM framework to spatially segment a pharmacological response based upon the temporal information. We have also applied this methodology to segment the response to cocaine (not shown), which has regionally variable kinetics (Marota et al., 2000). Although the spatial maps of the individual temporal components are compelling in terms of the anatomical distributions of signal changes, this methodology also has limitations.

Spatial segmentation of this type incurs a penalty in detection sensitivity in many regions relative to simple block comparisons

of temporal intervals, due to covariance among the multiple regressors. For example, the use of two regressors to describe the remifentanyl data decreased the global contrast to noise ratio by a factor of roughly two relative to use of a single regressor, but the latter analysis obviously provided a poor fit in many regions and failed to detect signal changes in certain areas due to biphasic responses. One factor that enabled high detection power in this study was the ability to average repeated injections, which requires a relatively short cerebral response that is repeatable. In general, responses to drugs may be neither stationary nor linear versus dose.

While the dominant temporal processes are clearly apparent, the basis functions determined by maximizing global CNR or minimizing global variance are not particularly unique because the cost functions vary slowly versus the shape of the regressors (e.g., Fig. 2a). For instance, the fast and slow components for the remifentanyl response can be made more similar without much change in global CNR. Thus, while the fast response magnitude in hippocampus will always exceed the fast response magnitude in caudate for any specification of basis functions using this simple gamma-variate form, it cannot be claimed with any certainty that the caudate does not possess some contribution from the fast component.

### Acknowledgments

The authors gratefully acknowledge financial support from the National Institute of Biomedical Imaging and Bioengineering (NIBIB, R01-EB001782-01) and the National Institute on Drug Abuse (NIDA, P01-DA09467B10, K08-DA14665-01). The authors thank Dr. Ralph Weissleder and Ms. Tina Balducci of the Center for Molecular Imaging Research at the Massachusetts General Hospital for synthesizing and distributing the MION contrast agent used in this study.

### References

- Barzo, P., Bari, F., Doczi, T., Jancso, G., Bodosi, M., 1993. Significance of the rate of systemic change in blood pressure on the short-term autoregulatory response in normotensive and spontaneously hypertensive rats. *Neurosurgery* 32, 611–618.
- Bloom, A.S., Hoffmann, R.G., Fuller, S.A., Pankiewicz, J., Harsch, H.H., Stein, E.A., 1999. Determination of drug-induced changes in functional MRI signal using a pharmacokinetic model. *Hum. Brain Mapp.* 8, 235–244.
- Borck, C., Jefferys, J.G., 1999. Seizure-like events in disinhibited ventral slices of adult rat hippocampus. *J. Neurophysiol.* 82, 2130–2142.
- Bowdle, T.A., 1998. Adverse effects of opioid agonists and agonist-antagonists in anaesthesia. *Drug Safety* 19, 173–189.
- Breiter, H., Gollub, R.L., Weisskoff, R.M., Kennedy, D., Makris, N., Berke, J., Goodman, J., Kantor, H., Gastfriend, D., Riorden, J., Mathew, T., Rosen, B., Hyman, S.E., 1997. Acute effects of cocaine on human brain activity and emotion. *Neuron* 19, 591–611.
- Buerkle, H., Yaksh, T.L., 1996. Comparison of the spinal actions of the mu-opioid remifentanyl with alfentanil and morphine in the rat. *Anesthesiology* 84, 94–102.
- Carroll, R.C., Beattie, E.C., von Zastrow, M., Malenka, R.C., 2001. Role of AMPA receptor endocytosis in synaptic plasticity. *Nat. Rev., Neurosci.* 2, 315–324.
- Chen, Y.C., Galpern, W.R., Brownell, A.L., Mathews, R.T., Bogdanov, M., Isacson, O., Keltner, J.R., Beal, M.F., Rosen, B.R., Jenkins, B.G., 1997. Detection of dopaminergic neurotransmitter activity using pharmacologic MRI: correlation with PET, microdialysis, and behavioral data. *Magn. Reson. Med.* 38, 389–398.
- Cohen, S.R., Kimes, A.S., London, E.D., 1991. Morphine decreases cerebral glucose utilization in limbic and forebrain regions while pain has no effect. *Neuropharmacology* 30, 125–134.
- Di Chiara, G., North, R.A., 1992. Neurobiology of opiate abuse. *Trends Pharmacol. Sci.* 13, 185–193.
- Diaz, A., Florez, J., Pazos, A., Hurle, M.A., 2000. Opioid tolerance and supersensitivity induce regional changes in the autoradiographic density of dihydropyridine-sensitive calcium channels in the rat central nervous system. *Pain* 86, 227–235.
- Drake, C.T., Milner, T.A., 1999. Mu opioid receptors are in somatodendritic and axonal compartments of GABAergic neurons in rat hippocampal formation. *Brain Res.* 849, 203–215.
- Ehlers, M.D., 2000. Reinsertion or degradation of AMPA receptors determined by activity-dependent endocytic sorting. *Neuron* 28, 511–525.
- Friston, K.J., Holmes, A.P., Worsley, K.J., Poline, J.P., Frith, C.D., Frackowiak, R.S.J., 1995. Statistical parametric maps in functional imaging: a general linear approach. *Hum. Brain Mapp.* 2, 189–210.
- Goodkin, H.P., Yeh, J.L., Kapur, J., 2005. Status epilepticus increases the intracellular accumulation of GABAA receptors. *J. Neurosci.* 25, 5511–5520.
- Haidar, S.H., Moreton, J.E., Liang, Z., Hoke, J.F., Muir, K.T., Eddington, N.D., 1997. Evaluating a possible pharmacokinetic interaction between remifentanyl and esmolol in the rat. *J. Pharm. Sci.* 86, 1278–1282.
- Hamilton, J.D., 1994. *Time Series Analysis*. Princeton Univ. Press.
- Hoge, R.D., Atkinson, J., Gill, B., Crelier, G.R., Marrett, S., Pike, G.B., 1999. Linear coupling between cerebral blood flow and oxygen consumption in activated human cortex. *Proc. Natl. Acad. Sci. U. S. A.* 96, 9403–9408.
- Holden, M., Hill, D.L., Denton, E.R., Jarosz, J.M., Cox, T.C., Rohlfing, T., Goodey, J., Hawkes, D.J., 2000. Voxel similarity measures for 3-D serial MR brain image registration. *IEEE Trans. Med. Imag.* 19, 94–102.
- Iadecola, C., 2004. Neurovascular regulation in the normal brain and in Alzheimer's disease. *Nat. Rev., Neurosci.* 5, 347–360.
- James, M.K., Feldman, P.L., Schuster, S.V., Bilotta, J.M., Brackeen, M.F., Leighton, H.J., 1991. Opioid receptor activity of GI 87084B, a novel ultra-short acting analgesic, in isolated tissues. *J. Pharmacol. Exp. Ther.* 259, 712–718.
- Johnson, L.A., Furman, C.A., Zhang, M., Guptaroy, B., Gnegy, M.E., 2005. Rapid delivery of the dopamine transporter to the plasmalemmal membrane upon amphetamine stimulation. *Neuropharmacology* 49, 750–758.
- Kalisch, R., Elbel, G.K., Gossel, C., Czisch, M., Auer, D.P., 2001. Blood pressure changes induced by arterial blood withdrawal influence bold signal in anesthetized rats at 7 Tesla: implications for pharmacologic MRI. *NeuroImage* 14, 891–898.
- Kneussel, M., 2002. Dynamic regulation of GABA(A) receptors at synaptic sites. *Brain Res. Brain Res. Rev.* 39, 74–83.
- Lambert, N.A., Harrison, N.L., Teyler, T.J., 1991. Evidence for mu opiate receptors on inhibitory terminals in area CA1 of rat hippocampus. *Neurosci. Lett.* 124, 101–104.
- Law, P.Y., Erickson, L.J., El-Kouhen, R., Dicker, L., Solberg, J., Wang, W., Miller, E., Burd, A.L., Loh, H.H., 2000. Receptor density and recycling affect the rate of agonist-induced desensitization of mu-opioid receptor. *Mol. Pharmacol.* 58, 388–398.
- Leppä, M., Korvenoja, A., Carlson, S., Timonen, P., Martinkauppi, S., Ahonen, J., Rosenberg, P.H., Aronen, H.J., Kalso, E., 2006. Acute opioid effects on human brain as revealed by functional magnetic resonance imaging. *NeuroImage* 31, 661–669.
- Leslie, R.A., James, M.F., 2000. Pharmacological magnetic resonance imaging: a new application for functional MRI. *Trends Pharmacol. Sci.* 21, 314–318.
- Lessard, A., Bachelard, H., 2002. Tonic inhibitory control exerted by opioid peptides in the paraventricular nuclei of the hypothalamus on regional hemodynamic activity in rats. *Br. J. Pharmacol.* 136, 753–763.
- Loscher, W., Ebert, U., 1996. The role of the piriform cortex in kindling. *Prog. Neurobiol.* 50, 427–481.

- Mandeville, J.B., Marota, J.J.A., Kosofsky, B.E., Keltner, J.R., Weissleder, R., Rosen, B.R., Weisskoff, R.M., 1998. Dynamic functional imaging of relative cerebral blood volume during rat forepaw stimulation. *Magn. Reson. Med.* 39, 615–624.
- Mandeville, J.B., Jenkins, B.G., Chen, Y.C., Choi, J.K., Kim, Y.R., Belen, D., Liu, C., Kosofsky, B.E., Marota, J.J., 2004. Exogenous contrast agent improves sensitivity of gradient-echo functional magnetic resonance imaging at 9.4 T. *Magn. Reson. Med.* 52, 1272–1281.
- Mandeville, J.B., Liu, C., Kosofsky, B.E., Marota, J.J., 2005. Transient signal changes in pharmacological fMRI: effects of no interest? *Proc. Int. Soc. Magn. Reson. Med.*, Miami, FL, p. 1512.
- Marota, J.J.A., Mandeville, J.B., Weisskoff, R.M., Moskowitz, M.A., Rosen, B.R., Kosofsky, B.E., 2000. Cocaine activation discriminates dopaminergic projections by temporal response: an fMRI study in rat. *NeuroImage* 11, 13–23.
- McQuiston, A.R., Saggau, P., 2003. Mu-opioid receptors facilitate the propagation of excitatory activity in rat hippocampal area CA1 by disinhibition of all anatomical layers. *J. Neurophysiol.* 90, 1936–1948.
- Mignat, C., Wille, U., Ziegler, A., 1995. Affinity profiles of morphine, codeine, dihydrocodeine and their glucuronides at opioid receptor subtypes. *Life Sci.* 56, 793–799.
- Moser, M.B., Moser, E.I., 1998. Functional differentiation in the hippocampus. *Hippocampus* 8, 608–619.
- Neumaier, J.F., Mailheau, S., Chavkin, C., 1988. Opioid receptor-mediated responses in the dentate gyrus and CA1 region of the rat hippocampus. *J. Pharmacol. Exp. Ther.* 244, 564–570.
- Panlilio, L.V., Schindler, C.W., 2000. Self-administration of remifentanyl, an ultra-short acting opioid, under continuous and progressive-ratio schedules of reinforcement in rats. *Psychopharmacology (Berlin)* 150, 61–66.
- Papatheodoropoulos, C., Moschovos, C., Kostopoulos, G., 2005. Greater contribution of *N*-methyl-D-aspartic acid receptors in ventral compared to dorsal hippocampal slices in the expression and long-term maintenance of epileptiform activity. *Neuroscience* 135, 765–779.
- Patel, S.S., Spencer, C.M., 1996. Remifentanyl. *Drugs* 52, 417–427 (discussion 428).
- Paxinos, G., Watson, C., 1998. *The Rat Brain in Stereotaxic Coordinates*. Academic Press, London.
- Rosow, C.E., Moss, J., Philbin, D.M., Savarese, J.J., 1982. Histamine release during morphine and fentanyl anesthesia. *Anesthesiology* 56, 93–96.
- Selley, D.E., Cao, C.C., Sexton, T., Schwegel, J.A., Martin, T.J., Childers, S. R., 2001. mu opioid receptor-mediated G-protein activation by heroin metabolites: evidence for greater efficacy of 6-monoacetylmorphine compared with morphine. *Biochem. Pharmacol.* 62, 447–455.
- Shah, Y.B., Haynes, L., Prior, M.J., Marsden, C.A., Morris, P.G., Chapman, V., 2005. Functional magnetic resonance imaging studies of opioid receptor-mediated modulation of noxious-evoked BOLD contrast in rats. *Psychopharmacology (Berlin)* 180, 761–773.
- Sotiriou, E., Papatheodoropoulos, C., Angelatou, F., 2005. Differential expression of gamma-aminobutyric acid-a receptor subunits in rat dorsal and ventral hippocampus. *J. Neurosci. Res.* 82, 690–700.
- Stefano, G.B., Hartman, A., Bilfinger, T.V., Magazine, H.I., Liu, Y., Casares, F., Goligorsky, M.S., 1995. Presence of the mu3 opiate receptor in endothelial cells. Coupling to nitric oxide production and vasodilation. *J. Biol. Chem.* 270, 30290–30293.
- Sun, S.Y., Liu, Z., Li, P., Ingenito, A.J., 1996. Central effects of opioid agonists and naloxone on blood pressure and heart rate in normotensive and hypertensive rats. *Gen. Pharmacol.* 27, 1187–1194.
- Tehrani, M.H., Barnes Jr., E.M., 1991. Agonist-dependent internalization of gamma-aminobutyric acidA/benzodiazepine receptors in chick cortical neurons. *J. Neurochem.* 57, 1307–1312.
- van Rijnsoever, C., Sidler, C., Fritschy, J.M., 2005. Internalized GABA-receptor subunits are transferred to an intracellular pool associated with the postsynaptic density. *Eur. J. Neurosci.* 21, 327–338.
- Vaughan, C.W., Ingram, S.L., Connor, M.A., Christie, M.J., 1997. How opioids inhibit GABA-mediated neurotransmission. *Nature* 390, 611–614.
- Wagner, J.J., Caudle, R.M., Chavkin, C., 1992. Kappa-opioids decrease excitatory transmission in the dentate gyrus of the guinea pig hippocampus. *J. Neurosci.* 12, 132–141.
- Wagner, K.J., Willoch, F., Kochs, E.F., Siessmeier, T., Tolle, T.R., Schwaiger, M., Bartenstein, P., 2001. Dose-dependent regional cerebral blood flow changes during remifentanyl infusion in humans: a positron emission tomography study. *Anesthesiology* 94, 732–739.
- Whitcher, B., Schwarz, A.J., Barjat, H., Smart, S.C., Grundy, R.I., James, M.F., 2005. Wavelet-based cluster analysis: data-driven grouping of voxel time courses with application to perfusion-weighted and pharmacological MRI of the rat brain. *NeuroImage* 24, 281–295.
- Worsley, K.J., Liao, C.H., Aston, J., Petre, V., Duncan, G.H., Morales, F., Evans, A.C., 2002. A general statistical analysis for fMRI data. *NeuroImage* 15, 1–15.
- Worsley, K.J., Taylor, J.E., Tomaiuolo, F., Lerch, J., 2004. Unified univariate and multivariate random field theory. *NeuroImage* 23 (Suppl. 1), S189–S195.
- Xi, Z.X., Wu, G., Stein, E.A., Li, S.J., 2002. GABAergic mechanisms of heroin-induced brain activation assessed with functional MRI. *Magn. Reson. Med.* 48, 838–843.
- Xie, C.W., Lewis, D.V., 1997. Involvement of cAMP-dependent protein kinase in mu-opioid modulation of NMDA-mediated synaptic currents. *J. Neurophysiol.* 78, 759–766.
- Xie, C.W., Morrisett, R.A., Lewis, D.V., 1992. Mu opioid receptor-mediated modulation of synaptic currents in dentate granule cells of rat hippocampus. *J. Neurophysiol.* 68, 1113–1120.
- Zaharchuk, G., Mandeville, J.B., Bogdonov Jr., A.A., Weissleder, R., Rosen, B.R., Marota, J.J.A., 1999. Cerebrovascular dynamics of autoregulation and hypotension: an MRI study of CBF and changes in total and microvascular cerebral blood volume during hemorrhagic hypotension. *Stroke* 30, 2197–2205.